



## **$\alpha$ -Cd<sub>13-x</sub>Sb<sub>10</sub> – the devil is in the details**

Sven Lidin, Simeon Ponou

### ► To cite this version:

Sven Lidin, Simeon Ponou.  $\alpha$ -Cd<sub>13-x</sub>Sb<sub>10</sub> – the devil is in the details. Journal of Inorganic and General Chemistry / Zeitschrift für anorganische und allgemeine Chemie, 2009, 635 (12), pp.1747. 10.1002/zaac.200900205 . hal-00493084

**HAL Id: hal-00493084**

<https://hal.science/hal-00493084>

Submitted on 18 Jun 2010

**HAL** is a multi-disciplinary open access archive for the deposit and dissemination of scientific research documents, whether they are published or not. The documents may come from teaching and research institutions in France or abroad, or from public or private research centers.

L'archive ouverte pluridisciplinaire **HAL**, est destinée au dépôt et à la diffusion de documents scientifiques de niveau recherche, publiés ou non, émanant des établissements d'enseignement et de recherche français ou étrangers, des laboratoires publics ou privés.



Zeitschrift für Anorganische und  
Allgemeine Chemie

### **a-Cd<sub>13-x</sub>Sb<sub>10</sub> – the devil is in the details**

Journal:	<i>Zeitschrift für Anorganische und Allgemeine Chemie</i>
Manuscript ID:	zaac.200900205.R1
Wiley - Manuscript type:	Article
Date Submitted by the Author:	28-Apr-2009
Complete List of Authors:	Lidin, Sven; Stockholm university Ponou, Simeon; Stockholm university, Inorganic Chemistry
Keywords:	thermoelectric, cadmium antimonide, cadmium deficiency



# $\alpha\text{-Cd}_{13-x}\text{Sb}_{10}$ – the devil is in the details

Simeon Ponou  
Sven Lidin

[Sven@inorg.su.se](mailto:Sven@inorg.su.se)

Inorganic Chemistry  
Arrhenius laboratory  
Stockholm University  
106 91 Stockholm  
Sweden

**Abstract**

A detailed study of the structure of  $\alpha\text{-Cd}_{13}\text{Sb}_{10}$  was performed using a high quality single crystal obtained from a Cd-rich melt. The study clearly shows that this sample is Cd-deficient, and should more properly be labelled  $\alpha\text{-Cd}_{13-x}\text{Sb}_{10}$ , but whether this is true in general for this phase, or if it is an effect of the precise conditions of synthesis remains unclear. Like for the similar Zn based compound, small differences in the Cd (Zn) content may be crucial in determining the electronic transport properties of the material.

## 1 2      Introduction 3

4      The discovery that the compound  $Zn_4Sb_3$  displays thermal transport properties akin to these of  
5      Perspex sparked a lot of interest in this unusual compound<sup>i</sup>, since bad transport properties is a  
6      good thing in a thermoelectric material. That interstitial zinc was responsible for the extreme  
7      transport behaviour was first suggested by Snyder *et al.*<sup>ii</sup> and in a sequence of studies  
8      Häußermann et al have conclusively proven the presence of interstitials in this system, as well  
9      as a number of different ordering schemes for these<sup>iii,iv,v</sup>. The importance of subtle changes in  
10     composition for the physical properties of the material has been pointed out by several  
11     authors<sup>vi vii viii ix</sup>. While the phase diagram of Zn-Sb is relatively rich, the Cd-Sb system  
12     contains only one stable phase, the equimolar CdSb, but on the Cd rich side of the phase  
13     diagram a number of phases may be formed with relative facility either from by  
14     undercooling the binary melt or from ternary fluxes with Bi, Sn or In. At least two distinct  
15     compounds can be made this way,  $Cd_4Sb_3$  and  $Cd_3Sb_2$ , both showing temperature dependent  
16     polymorphism. We recently reported on the synthesis, structural elucidation and properties  
17     measurements of the two polymorphs of  $Cd_4Sb_3$ , the high temperature phase  $\beta$ - $Cd_4Sb_3$  and the  
18     room temperature phase  $\alpha$ - $Cd_4Sb_3$ <sup>x</sup>. The phase transition temperature depends significantly on  
19     the flux, for a quenched binary sample the  $\alpha \rightarrow \beta$  transformation temperature was 375 K, for  
20     a Sn flux grown sample the transition temperature was depressed to just above 360 K and for  
21     a Bi flux grown sample the transition took place below 360 K. The hysteresis was also quite  
22     different for the three samples, for the binary melt quenched sample and the Bi flux grown  
23     sample the heating and cooling transitions differed by about 5 K in temperature, but for the Sn  
24     grown sample, the difference is more than 25 K, even though the Sn content as measured by  
25     electron microprobe analysis is less than 0.1 %. The Cd/Sb balance in the samples shows  
26     small differences, but lie close to the crystallographic composition of the  $\alpha$  phase,  $Cd_{13}Sb_{10}$ .  
27

28     The phase transition is caused by the ordering of interstitial Cd positions. This ordering causes  
29     some regular Cd sites (corresponding to Wyckoff position 36f in the trigonal  $\beta$  phase cell) to  
30     be vacated. In the corresponding Zn based system, we have found that the  $\alpha$ -phase is not fully  
31     ordered, but that the ordered Zn interstitials are partially unoccupied, and the vacation of the  
32     corresponding regular sites is also incomplete.  
33

34     The single crystal structural study of the melt quenched sample allowed for the solution of the  
35      $\alpha$ - $Cd_4Sb_3$  phase super structure, but all attempts to locate residual electron density  
36     corresponding to incomplete vacation of regular sites were unsuccessful. The quality of the  
37     single crystal refinement was however limited by the quality of the single crystal specimen,  
38     and in order to further investigate possible occupational disorder in  $\alpha$ - $Cd_4Sb_3$  we therefore  
39     pursued a number of different synthetic procedures in order to grow better quality single  
40     crystals that might allow a high quality refinement.  
41

## 42      Experimental 43

### 44      Synthesis

45      A single crystal of the title compound was obtained from a Cd rich melt. A mixture of  
46      approximately 1 g of the elements (Cd, 99.9% and Sb, 99.5%; all purchased from Sigma-  
47      Aldrich) with the weight ratio Cd:Sb = 0.65:0.40 was loaded in a steel ampoule which was  
48      weld-sealed at both ends under argon atmosphere. The sample was first placed vertically in a  
49      muffle oven and heated at 923 K. Then, the ampoule was turned to a horizontal position and  
50      the oven temperature was cooled down to 673 K where the sample was subsequently annealed  
51  
52  
53  
54  
55  
56  
57  
58  
59  
60

1  
2 for about 48 hours. Finally, the sample was removed from the furnace and allowed to cool  
3 down to room temperature.  
4

5 *Single crystal X-ray diffraction*  
6

7 A suitable crystal was picked from the crushed sample, mounted on a glass fibre and  
8 diffraction data was measured on an Oxford Diffraction XCalibur 3 CCD diffractometer with  
9 MoKa radiation ( $\lambda=0.71073\text{\AA}$ ). 50kV, 40mA). Two data sets were acquired at room  
10 temperature 295 K and at 100 K using an Oxford cryostream system. The data reduction was  
11 performed using the Oxford diffraction Crysaliis system, and the refinement was carried out  
12 using the JANA2000 program<sup>xi</sup>. All details of the measurements are given in tables 1 and  
13 2. The monoclinic super structure cell is obvious in the diffraction pattern, but the small  
14 crystal chosen exhibits less obvious twinning than expected, and picking out a dominant  
15 domain was straight-forward. In figure 1 the twinning pattern is indicated. As indicated, the  
16 diffraction pattern consists of two distinct sets. The basic reflections of the  $\beta$ -phase are  
17 common to all individuals, while the satellites are unique to each of the three domain  
18 orientations in the twinned structure. The data is therefore readily deconvoluted, although  
19 absolute intensity information is available only after the structure is solved and refined. In  
20 practise, as explained in previous work, to solve the structure a model featuring the  $\beta$ -phase in  
21 the setting of the monoclinic unit cell and embellished with a number of interstitial positions  
22 identified as noticeable in the electron density map of the solution from the  $\beta$ -phase was used  
23 as a starting set. This model was then refined by allowing parial occupancy for any atoms that  
24 had neighbours at unphysically short distances. After a number of least squares refinement  
25 cycles, positions with an occupancy below a threshold value were discarded, the difference  
26 electron density map was evaluated to identify new possible interstitial positions, and the  
27 distance map was re-evaluated to identify which positions that should be refined in terms of  
28 occupancy. The threshold value was adjusted during the refinement to yield increasingly hard  
29 conditions for considering a position as empty. This solution strategy was used in the maximal  
30 monoclinic subgroups to  $R-3c$ ,  $P2_1/n$ , and subsequently in the three subgroups  $Pn$ ,  $P2_1$ , and  $P-1$ .  
31 A satisfactory convergence was achievable only in  $Pn$ . The structure in space group  $Pn$   
32 from previous work was used as a starting model with 60 independent Sb positions and 78  
33 independent Cd positions. The Sb atoms were grouped in two sets (A and B) according to  
34 their positions in the  $\beta$  phase structure. The Cd positions were also grouped in two sets, a first,  
35 larger, set of 64 Cd positions (A) corresponding to the 36f position in the  $\beta$  phase, and one  
36 grouping consisting of the 14 ordered interstitial Cd positions (B). Within these groups each  
37 set was modelled using a single, isotropic, thermal displacement parameter. After  
38 convergence of this refinement, the difference electron density map was examined for  
39 prominent residuals, and the positions of these were compared to, and found to correspond to,  
40 those of the vacated regular Cd positions. A new set (C) of these 8 positions were included as  
41 partially occupied in a modified model, and the occupancy of the 14 Cd positions in group B  
42 corresponding to the ordered interstitials was reduced by the same amount. In the ensuing  
43 cycles of refinement the occupancies of these two groups were coupled complementarily.  
44 Since the 8 new positions correspond to the 36f position in the  $\beta$  phase, the isotropic thermal  
45 displacement parameter of group CdC was set equal to that of set CdA. All pertinent  
46 parameters for the x ray study are given in table 1 and 2. Final positional and occupational  
47 parameters are given in tables 3 and 4.

48  
49 **Results and discussion**  
50  
51  
52  
53  
54  
55  
56  
57  
58  
59  
60

Formatted: Font: Symbol

Formatted: Font: Symbol

Formatted: Font: Symbol

Formatted: Font: Italic

Formatted: Font: Italic

Formatted: Font: Italic, Subscript

Formatted: Font: Italic

Formatted: Font: Italic

Formatted: Font: Italic

Formatted: Font: Italic

The results of the refinements, both for the data collected at ambient temperature and for the data from 100 K largely agree with the results previously published, but with two important exceptions. First, the quality of the crystal, and hence the data is far superior in this measurement compared to that of the crystals used earlier, and this is also clear from the final agreement between model and data. The number of observed reflections is lower, as a result of the smaller sample size, but the parameter-to-data ratio is still close to 10 even for the observed ( $F^2 > 3\sigma(F^2)$ ) set. The volumes of the minor twin constituents were about 1/8 each, adding up to 1/4 of the total crystal volume. The twinning matrices were as reported earlier

11	0.5000	-1.0000	1.5000
12	0.2500	-0.5000	-0.7500
13	0.3333	0.6667	0.0000
14			
15	0.4971	1.0000	1.5000
16	-0.2500	-0.5000	0.7500
17	0.3333	-0.6667	0.0000

As shown earlier, the ordered interstitials form chains along the monoclinic a-axis. In figure 2a, the relative positions of these chains are shown in a projection parallel to a. Sb atoms are shown in blue, set A of the Cd atoms is shown in yellow, set B in red and set C in green. It is evident that the chains are well separated and that the deformation of the surrounding structure is negligible. A view down the monoclinic c-axis (fig 2b) is ideal for displaying the structure of the chain of interstitials. In this view, the atomic positions of set SbA and SbB and set CdA have been removed from the top of the image to display the chain of interstitials of group CdB and the alternative positions of group CdC more clearly. Finally, in the image 2c, where the structure is projected down the b-axis, the lamellar nature of the structure is shown. An alternation between two filled and one empty lamella is obvious, and this is clearly the reason for the 3-fold superstructure along c.

Deleted: 1

Deleted: 1

Deleted: 1

The reduction in Cd content, x, generated by the partial exchange of the 14 atomic positions in group CdB for the 8 positions in group CdC is given by  $Cd(A)_{64}Cd(B)_{14(1-x)}Cd(C)_8Sb(A,B)_{60}$  which simplifies to  $Cd_{13-x}Sb_{10}$ . In the final refinement, the deficiency on the occupancy of set CdC converges to about 20%. This means that the Cd content is reduced to  $Cd_{12.8}Sb_{10}$ , or from 56.5% to 56.1%, equivalent to about two esd. in the electron microprobe analysis. The failure to locate significant electron density on positions corresponding to set CdC in our previous work may be taken as an indication that this product was in fact stoichiometric  $Cd_{13}Sb_{10}$ , but as mentioned in the introduction, it may equally well simply reflect the quality of the single crystal. It should be noted that weak super structure ordering combined with twinning places rather high demands on crystal quality for detailed analysis. We therefore cannot say with any certainty that the two samples really differ in composition, but there are certainly good reasons to assume that a certain composition range is permissible for  $Cd_4Sb_3$ . The crystal used in this study has a unit cell volume that is 0.2% smaller (at ambient conditions and 0.1% at 100K) than that used in the previous study. The significance of this difference is debatable, and it is in fact larger than would be expected from the Cd deficiency alone. The fact that the phase may be grown from a rather extended region, compositionally as well as in temperature, and that the phase originally formed is the disordered  $\beta$ -phase certainly leaves room for compositional variations. The local structure of  $\alpha$ - $Cd_4Sb_3$  comprising lamellae containing ordered interstitials interleaved with lamellae devoid of interstitial positions certainly offers a facile way to structurally accommodate a slight variation in under-occupancy of Cd. This is indeed the case for the analogous  $Zn_4Sb_3$

1 compound which further strengthens the suspicion. A last important indication is the report by  
2 Zelinska<sup>xii</sup> of a Cd<sub>4</sub>Sb<sub>3</sub> quenched from the binary melt that doesn't exhibit any super structure  
3 ordering at room temperature. This would be most easily understood in terms of small  
4 compositional variations determining the transition temperature between the  $\alpha$  and  $\beta$  forms of  
5 this phase.  
6

## 7 Conclusion

8 **Formatted:** Font: Bold

9 Ths  $\alpha$ -phase structure of Cd<sub>13</sub>Sb<sub>10</sub> from a new synthetic protocol was unambiguously shown  
10 to be Cd deficient, *i.e.*, the compound is Cd<sub>13-x</sub>Sb<sub>10</sub>. This does not mean that previous studies  
11 by us and others indicating a stoichiometric  $\alpha$ -phase, or even a room temperature  $\beta$ -phase are  
12 in error. To the contrary, we think it indicates a compositional variability within certain  
13 bounds that allows for a Cd-poor sample to remain in the  $\beta$ -phase throughout the entire  
14 temperature range of the investigation, or to display various degrees of  $\alpha$ / $\beta$ -polysynthetic  
15 behaviour. As for the compound Zn<sub>13</sub>Sb<sub>10</sub>, the  $\alpha$ -phase super structure displays a clear layer  
16 structure that allows for the facile intergrowth between the two phases. The fact that the Cd  
17 compound only forms as a meta stable compound from the melt make detailed investigations  
18 of compositional and temporal parameters difficult. Slow cooling of a melt always results in  
19 elemental Cd and the 1:1 compound.  
20

21 **Formatted:** Font: Symbol

22 **Formatted:** Font: Italic

23 **Formatted:** Font: Symbol

24 **Formatted:** Font: Symbol

25 **Formatted:** Font: Symbol

26 **Formatted:** Font: Symbol

27 **Formatted:** Font: Symbol

28 **Formatted:** Font: Symbol

## 29 Acknowledgement

30 **Formatted:** Font: Bold

31 Financial support from the Swedish research council and the Wennergren Foundation (post  
32 doc financing for S.P.) is gratefully acknowledged. This work is part of the effort within the  
33 CMA European project.  
34  
35  
36  
37  
38  
39  
40  
41  
42  
43  
44  
45  
46  
47  
48  
49  
50  
51  
52  
53  
54  
55  
56  
57  
58  
59  
60

Figure captions1

Scheme of the twinned diffraction pattern. The reflections marked by red circles are main reflections from the high temperature b-phase, while those marked by yellow circles generate the superstructure. Every red reflection is part of three twin lattices as indicated for the set along the c\* axis by the three intersection planes.

2

The structure of the compound Cd<sub>13-x</sub>Sb<sub>10</sub> in axial projection. Sb positions are shown in blue, regular Zn positions in yellow, ordered interstitial Zn positions are shown in red and finally partially occupied regular Zn in green. a) view down a-axis, b) view down c-axis, c) view down b-axis

**Formatted:** Subscript

Table 1

*Crystal data*

<u>Cd<sub>153.662</sub>Sb<sub>120</sub></u>	$V = 7643.2 (5) \text{ \AA}^3$
$M_r = 31883.1$	$Z = 1$
<u>Monoclinic, Pn</u>	<u>Mo K<math>\alpha</math></u>
$a = 11.4478 (4) \text{ \AA}$	$\mu = 20.81 \text{ mm}^{-1}$
$b = 26.0793 (7) \text{ \AA}$	$T = 293 \text{ K}$
$c = 26.0691 (10) \text{ \AA}$	$0.10 \times 0.05 \times 0.03 \text{ mm}$
$\beta = 100.872 (4)^\circ$	

*Data collection*

XCalibur 3 diffractometer	42170 independent reflections
Absorption correction: Gaussian <u>CrysAlis RED, Oxford Diffraction Ltd.,</u> <u>Version 1.171.32.9 (release 17-07-2007)</u> <u>CrysAlis171 .NET (compiled Aug 17</u> <u>2007,17:36:27) Numerical absorption</u> <u>correction based on Gaussian integration over</u> <u>a multifaceted crystal model</u>	2407 reflections with $I > 3\sigma(I)$
$T_{\min} = 0.288, T_{\max} = 0.656$	$R_{\text{int}} = 0.175$
72678 measured reflections	

Deleted: g

*Refinement*

$R[F^2 > 2\sigma(F^2)] = 0.038$	$\Delta\rho_{\max} = 5.10 \text{ e \AA}^{-3}$
$wR(F^2) = 0.070$	$\Delta\rho_{\min} = -3.82 \text{ e \AA}^{-3}$
$S = 0.50$	
42170 reflections	445 parameters

Table 2

*Crystal data*

<u>Cd<sub>154.036</sub>Sb<sub>120</sub></u>	$V = 7636.3 (5) \text{ \AA}^3$
$M_r = 31925.2$	$Z = 1$
<u>Monoclinic, Pn</u>	<u>Mo K<math>\alpha</math></u>
$a = 11.4469 (4) \text{ \AA}$	$\mu = 20.85 \text{ mm}^{-1}$
$b = 26.0624 (9) \text{ \AA}$	$T = 100 \text{ K}$
$c = 26.0579 (10) \text{ \AA}$	$0.10 \times 0.05 \times 0.03 \text{ mm}$
$\beta = 100.797 (3)^\circ$	

*Data collection*

<u>XCalibur 3</u> <u>diffractometer</u>	<u>42010</u> independent reflections
Absorption correction: <u>Gaussian</u> <u>CrysAlis RED, Oxford Diffraction Ltd.,</u> <u>Version 1.171.32.9 (release 17-07-2007)</u> <u>CrysAlis171 .NET (compiled Aug 17</u> <u>2007,17:36:27) Numerical absorption</u> <u>correction based on Gaussian integration over</u> <u>a multifaceted crystal model</u>	<u>3243</u> reflections with $I > 3\sigma(I)$
$T_{\min} = 0.288$ , $T_{\max} = 0.656$	$R_{\text{int}} = 0.144$
<u>72229</u> measured reflections	

*Refinement*

$R[F^2 > 2\sigma(F^2)] = 0.037$	$\Delta\rho_{\max} = 5.46 \text{ e \AA}^{-3}$
$wR(F^2) = 0.069$	$\Delta\rho_{\min} = -4.78 \text{ e \AA}^{-3}$
$S = 0.56$	
<u>42010</u> reflections	<u>445</u> parameters

Table 3

Fractional atomic coordinates and isotropic or equivalent isotropic displacement parameters (Å<sup>2</sup>) at T=293K

	x	y	z	$U_{\text{iso}}^*/U_{\text{eq}}$	Occ. (<1)
Sba1	1.600263	0.8777 (3)	0.692587	0.02009 (10)*	
Sba2	2.0982 (12)	0.6292 (3)	0.6974 (4)	0.02009 (10)*	
Sba3	1.5962 (11)	0.8729 (3)	0.3664 (4)	0.02009 (10)*	
Sba4	1.6062 (12)	0.6167 (3)	0.8571 (5)	0.02009 (10)*	
Sba5	2.0964 (11)	0.8745 (3)	0.5277 (4)	0.02009 (10)*	
Sba6	2.1017 (13)	1.1259 (3)	0.3592 (5)	0.02009 (10)*	
Sba7	1.1013 (13)	0.6213 (3)	1.0323 (5)	0.02009 (10)*	
Sba8	1.5956 (13)	1.1247 (3)	0.5280 (5)	0.02009 (10)*	
Sba9	1.1033 (11)	1.3728 (3)	0.5282 (4)	0.02009 (10)*	
Sba10	1.5982 (10)	1.3637 (3)	0.3606 (4)	0.02009 (10)*	
Sba11	1.0973 (13)	1.1193 (3)	0.6947 (5)	0.02009 (10)*	
Sba12	1.3807 (12)	0.6231 (3)	0.7893 (4)	0.02009 (10)*	
Sba13	1.3813 (11)	1.1247 (3)	0.4551 (4)	0.02009 (10)*	
Sba14	1.3831 (12)	0.8791 (3)	0.6245 (4)	0.02009 (10)*	
Sba15	1.3800 (12)	1.3705 (3)	0.2873 (4)	0.02009 (10)*	
Sba16	1.8832 (11)	0.6267 (3)	0.6249 (4)	0.02009 (10)*	
Sba17	1.8843 (9)	0.8745 (3)	0.4535 (3)	0.02009 (10)*	
Sba18	0.8834 (12)	1.1220 (3)	0.6172 (4)	0.02009 (10)*	
Sba19	0.8837 (11)	0.6151 (3)	0.9580 (4)	0.02009 (10)*	
Sba20	1.3816 (12)	0.8706 (3)	0.2885 (4)	0.02009 (10)*	
Sba21	0.8806 (12)	1.3733 (3)	0.4593 (4)	0.02009 (10)*	
Sba22	1.3815 (12)	0.3759 (3)	0.6222 (4)	0.02009 (10)*	
Sba23	1.8804 (11)	1.1250 (3)	0.2872 (4)	0.02009 (10)*	
Sba24	1.6003 (11)	0.3807 (3)	0.6941 (4)	0.02009 (10)*	
Sbb25	1.8167 (11)	0.5377 (3)	0.7736 (4)	0.01987 (9)*	
Sbb26	1.6743 (11)	0.7129 (3)	0.7077 (4)	0.01987 (9)*	

1	Sbb27	1.4969 (11)	0.9485 (3)	0.4895 (4)	0.01987 (9)*	
2	Sbb28	1.3117 (11)	1.2791 (3)	0.4480 (4)	0.01987 (9)*	
3	Sbb29	1.3223 (11)	0.7184 (3)	0.6133 (4)	0.01987 (9)*	
4	Sbb30	1.8090 (11)	0.9618 (3)	0.6062 (4)	0.01987 (9)*	
5	Sbb31	1.4919 (11)	0.5469 (3)	0.9904 (4)	0.01987 (9)*	
6	Sbb32	2.1671 (12)	0.5360 (3)	0.8715 (4)	0.01987 (9)*	
7	Sbb33	1.9907 (11)	0.8012 (3)	0.6580 (4)	0.01987 (9)*	
8	Sbb34	1.3112 (11)	0.7900 (3)	0.7744 (4)	0.01987 (9)*	
9	Sbb35	1.3192 (11)	1.2096 (3)	0.6036 (4)	0.01987 (9)*	
10	Sbb36	1.9919 (11)	0.6965 (3)	0.8241 (4)	0.01987 (9)*	
11	Sbb37	1.9891 (12)	1.2953 (3)	0.3255 (4)	0.01987 (9)*	
12	Sbb38	1.4955 (11)	0.5579 (3)	0.6544 (4)	0.01987 (9)*	
13	Sbb39	0.9938 (11)	1.1950 (3)	0.4913 (4)	0.01987 (9)*	
14	Sbb40	2.1658 (11)	0.5420 (3)	0.5434 (4)	0.01987 (9)*	
15	Sbb41	1.6738 (11)	0.7818 (3)	0.5409 (4)	0.01987 (9)*	
16	Sbb42	1.2950 (10)	0.7154 (3)	0.9510 (4)	0.01987 (9)*	
17	Sbb43	1.4909 (11)	1.0487 (3)	0.6549 (4)	0.01987 (9)*	
18	Sbb44	1.4951 (11)	0.4545 (3)	0.8217 (4)	0.01987 (9)*	
19	Sbb45	1.8183 (11)	1.0380 (3)	0.4372 (4)	0.01987 (9)*	
20	Sbb46	1.6787 (11)	0.7815 (3)	0.8702 (4)	0.01987 (9)*	
21	Sbb47	1.4909 (11)	1.0550 (3)	0.3223 (4)	0.01987 (9)*	
22	Sbb48	2.1601 (11)	0.9688 (3)	0.7012 (4)	0.01987 (9)*	
23	Sbb49	1.6683 (11)	1.2887 (3)	0.5417 (4)	0.01987 (9)*	
24	Sbb50	1.7974 (11)	0.9584 (3)	0.2783 (4)	0.01987 (9)*	
25	Sbb51	1.8153 (11)	0.4652 (3)	0.9497 (4)	0.01987 (9)*	
26	Sbb52	0.9932 (12)	1.3038 (3)	0.6564 (4)	0.01987 (9)*	
27	Sbb53	1.4917 (12)	1.4504 (3)	0.4913 (4)	0.01987 (9)*	
28	Sbb54	2.1655 (11)	0.9591 (3)	0.3790 (4)	0.01987 (9)*	
29	Sbb55	1.8089 (11)	0.4615 (3)	0.6094 (4)	0.01987 (9)*	
30	Sbb56	2.1619 (11)	0.4642 (3)	0.7057 (4)	0.01987 (9)*	

1	Sbb57	2.1638 (11)	1.0324 (3)	0.5334 (4)	0.01987 (9)*	
2	Sbb58	1.6753 (11)	1.2133 (3)	0.7063 (4)	0.01987 (9)*	
3	Sbb59	1.6725 (11)	1.2115 (3)	0.3716 (4)	0.01987 (9)*	
4	Sbb60	1.8147 (12)	1.0348 (3)	0.7778 (4)	0.01987 (9)*	
5	Cda1	1.5679 (13)	0.7974 (4)	0.7613 (5)	0.02839 (9)*	
6	Cda2	2.1032 (13)	0.7285 (3)	0.7347 (5)	0.02839 (9)*	
7	Cda3	2.0595 (12)	0.5515 (3)	0.7643 (5)	0.02839 (9)*	
8	Cda4	1.6164 (13)	0.9734 (4)	0.4042 (5)	0.02839 (9)*	
9	Cda5	1.5663 (13)	1.2033 (4)	0.5948 (5)	0.02839 (9)*	
10	Cda6	1.7664 (12)	0.6496 (3)	0.7971 (5)	0.02839 (9)*	
11	Cda7	2.0617 (13)	1.0474 (3)	0.4263 (5)	0.02839 (9)*	
12	Cda8	1.6172 (13)	0.5225 (4)	0.9039 (5)	0.02839 (9)*	
13	Cda9	1.1013 (12)	1.2708 (3)	0.5687 (5)	0.02839 (9)*	
14	Cda10	2.0589 (12)	0.9520 (3)	0.5930 (5)	0.02839 (9)*	
15	Cda11	1.6086 (13)	1.0247 (4)	0.5672 (5)	0.02839 (9)*	
16	Cda12	1.7661 (13)	0.8540 (4)	0.6303 (5)	0.02839 (9)*	
17	Cda13	1.7696 (13)	1.1468 (4)	0.4662 (5)	0.02839 (9)*	
18	Cda14	1.6101 (13)	0.4800 (4)	0.7313 (5)	0.02839 (9)*	
19	Cda15	1.4246 (13)	0.6991 (3)	0.7217 (5)	0.02839 (9)*	
20	Cda16	1.8687 (13)	0.7759 (4)	0.7450 (5)	0.02839 (9)*	
21	Cda17	1.5726 (13)	0.7948 (3)	0.4358 (5)	0.02839 (9)*	
22	Cda18	1.2557 (12)	1.0988 (3)	0.6214 (4)	0.02839 (9)*	
23	Cda19	1.3785 (12)	0.4754 (4)	0.9130 (5)	0.02839 (9)*	
24	Cda20	1.5655 (12)	1.2935 (3)	0.4333 (5)	0.02839 (9)*	
25	Cda21	1.3818 (12)	1.0232 (3)	0.4170 (5)	0.02839 (9)*	
26	Cda22	1.2474 (11)	0.5825 (3)	0.9694 (4)	0.02839 (9)*	
27	Cda23	1.0689 (12)	0.5446 (3)	1.1028 (5)	0.02839 (9)*	
28	Cda24	2.2705 (12)	0.6070 (4)	0.6318 (5)	0.02839 (9)*	
29	Cda25	1.2728 (13)	1.3942 (3)	0.4650 (5)	0.02839 (9)*	
30	Cda26	1.7486 (12)	1.3426 (3)	0.2909 (5)	0.02839 (9)*	

1	Cda27	2.2764 (13)	0.8944 (3)	0.4704 (4)	0.02839 (9)*	
2	Cda28	0.8649 (12)	1.2231 (3)	0.5745 (4)	0.02839 (9)*	
3	Cda29	2.1166 (13)	1.2242 (4)	0.4057 (5)	0.02839 (9)*	
4	Cda30	1.7174 (13)	0.6045 (4)	0.6877 (5)	0.02839 (9)*	
5	Cda31	1.9198 (12)	0.5373 (3)	0.8816 (4)	0.02839 (9)*	
6	Cda32	2.1166 (12)	0.7753 (3)	0.5705 (4)	0.02839 (9)*	
7	Cda33	1.3638 (12)	0.9737 (3)	0.5729 (4)	0.02839 (9)*	
8	Cda34	1.9123 (12)	0.9546 (4)	0.3883 (5)	0.02839 (9)*	
9	Cda35	1.2073 (12)	1.1410 (3)	0.5137 (4)	0.02839 (9)*	
10	Cda36	2.2152 (13)	0.6458 (4)	0.8537 (5)	0.02839 (9)*	
11	Cda37	1.7191 (13)	0.8947 (4)	0.5208 (5)	0.02839 (9)*	
12	Cda38	1.3701 (12)	0.5255 (4)	0.7400 (5)	0.02839 (9)*	
13	Cda39	1.9150 (12)	0.4637 (3)	0.7151 (5)	0.02839 (9)*	
14	Cda40	1.4207 (13)	1.2976 (3)	0.5535 (5)	0.02839 (9)*	
15	Cda41	1.6142 (13)	0.9748 (4)	0.7366 (5)	0.02839 (9)*	
16	Cda42	1.8776 (13)	1.2699 (4)	0.4192 (5)	0.02839 (9)*	
17	Cda43	2.2140 (12)	0.8580 (3)	0.6873 (5)	0.02839 (9)*	
18	Cda44	1.9150 (12)	1.0400 (3)	0.5477 (5)	0.02839 (9)*	
19	Cda45	1.0648 (13)	1.4509 (3)	0.5971 (5)	0.02839 (9)*	
20	Cda46	1.2366 (11)	0.6634 (3)	0.5224 (4)	0.02839 (9)*	
21	Cda47	1.1125 (12)	0.7252 (3)	1.0707 (4)	0.02839 (9)*	
22	Cda48	1.2266 (12)	1.3472 (3)	0.3536 (5)	0.02839 (9)*	
23	Cda49	2.2784 (12)	1.1084 (3)	0.2944 (5)	0.02839 (9)*	
24	Cda50	1.0645 (12)	1.0453 (3)	0.7667 (5)	0.02839 (9)*	
25	Cda51	1.3816 (12)	0.5230 (3)	1.0874 (5)	0.02839 (9)*	
26	Cda52	1.7112 (12)	0.8902 (3)	0.1897 (5)	0.02839 (9)*	
27	Cda53	1.4242 (13)	1.2023 (4)	0.3862 (5)	0.02839 (9)*	
28	Cda54	1.7482 (12)	0.8369 (3)	0.2999 (5)	0.02839 (9)*	
29	Cda55	1.7735 (12)	0.3541 (3)	0.6282 (5)	0.02839 (9)*	
30	Cda56	1.7296 (12)	0.4035 (3)	0.8602 (5)	0.02839 (9)*	

1	Cda57	1.7094 (12)	1.1054 (4)	0.3530 (5)	0.02839 (9)*	
2	Cda58	1.8701 (13)	1.2277 (4)	0.2421 (5)	0.02839 (9)*	
3	Cda59	1.9094 (12)	0.9587 (3)	0.7131 (5)	0.02839 (9)*	
4	Cda60	1.3747 (12)	0.4761 (3)	0.5834 (5)	0.02839 (9)*	
5	Cda61	1.7216 (12)	1.4008 (3)	0.5192 (5)	0.02839 (9)*	
6	Cda62	1.9190 (12)	0.5449 (3)	0.5568 (5)	0.02839 (9)*	
7	Cda63	1.7265 (12)	1.0975 (3)	0.6842 (5)	0.02839 (9)*	
8	Cda64	1.4328 (12)	0.8010 (3)	0.5562 (5)	0.02839 (9)*	
9	Cdb65	0.9529 (12)	1.2065 (4)	0.7069 (5)	0.0212 (5)*	0.805 (3)
10	Cdb66	1.5262 (12)	0.3475 (3)	0.7911 (4)	0.0212 (5)*	0.805 (3)
11	Cdb67	1.5442 (13)	0.9573 (4)	0.2759 (5)	0.0212 (5)*	0.805 (3)
12	Cdb68	1.2434 (11)	0.2043 (3)	0.7116 (4)	0.0212 (5)*	0.805 (3)
13	Cdb69	1.4934 (11)	0.1482 (3)	0.7061 (4)	0.0212 (5)*	0.805 (3)
14	Cdb70	1.4621 (11)	0.2756 (3)	0.6976 (4)	0.0212 (5)*	0.805 (3)
15	Cdb71	1.0437 (13)	0.7074 (4)	0.9445 (5)	0.0212 (5)*	0.805 (3)
16	Cdb72	1.4513 (13)	1.4564 (4)	0.3740 (5)	0.0212 (5)*	0.805 (3)
17	Cdb73	1.5278 (11)	0.6524 (3)	0.9598 (4)	0.0212 (5)*	0.805 (3)
18	Cdb74	1.4833 (12)	0.8499 (4)	0.8707 (4)	0.0212 (5)*	0.805 (3)
19	Cdb75	1.4641 (11)	0.7242 (3)	0.8671 (4)	0.0212 (5)*	0.805 (3)
20	Cdb76	1.2544 (11)	0.8006 (3)	0.8860 (4)	0.0212 (5)*	0.805 (3)
21	Cdb77	1.2713 (12)	0.9712 (4)	0.2909 (5)	0.0212 (5)*	0.805 (3)
22	Cdb78	1.2736 (12)	0.5282 (3)	0.4594 (4)	0.0212 (5)*	0.805 (3)
23	Cdc79	-1.491 (3)	0.6737 (12)	-0.0717 (12)	0.020 (3)*	0.195 (3)
24	Cdc80	-1.510 (3)	0.2921 (10)	-0.2642 (11)	0.020 (3)*	0.195 (3)
25	Cdc81	-1.228 (3)	1.0627 (10)	0.1363 (11)	0.020 (3)*	0.195 (3)
26	Cdc82	-1.152 (3)	0.2624 (11)	-0.2267 (12)	0.020 (3)*	0.195 (3)
27	Cdc83	1.668 (3)	1.0232 (11)	0.2107 (12)	0.020 (3)*	0.195 (3)
28	Cdc84	0.445 (3)	0.8213 (12)	0.8604 (12)	0.020 (3)*	0.195 (3)
29	Cdc85	0.443 (3)	0.5325 (10)	0.3500 (11)	0.020 (3)*	0.195 (3)
30	Cdc86	0.197 (4)	0.7797 (15)	0.8615 (16)	0.020 (3)*	0.195 (3)

Table 4

Fractional atomic coordinates and isotropic or equivalent isotropic displacement parameters  
(Å<sup>2</sup>)

	<i>x</i>	<i>y</i>	<i>z</i>	<i>U</i> <sub>iso</sub> */* <i>U</i> <sub>eq</sub>	Occ. (<1)
Sb1_1	1.600263	0.8787 (3)	0.692587	0.00971 (9)*	
Sb1_2	2.1016 (11)	0.6281 (3)	0.6908 (4)	0.00971 (9)*	
Sb1_3	1.6020 (10)	0.8707 (3)	0.3601 (4)	0.00971 (9)*	
Sb1_4	1.6033 (11)	0.6184 (3)	0.8548 (4)	0.00971 (9)*	
Sb1_5	2.1013 (10)	0.8724 (3)	0.5231 (4)	0.00971 (9)*	
Sb1_6	2.1013 (11)	1.1274 (3)	0.3551 (4)	0.00971 (9)*	
Sb1_7	1.1033 (11)	0.6225 (3)	1.0285 (5)	0.00971 (9)*	
Sb1_8	1.5946 (10)	1.1261 (3)	0.5216 (4)	0.00971 (9)*	
Sb1_9	1.1053 (10)	1.3725 (3)	0.5243 (4)	0.00971 (9)*	
Sb1_10	1.6009 (9)	1.3639 (2)	0.3562 (4)	0.00971 (9)*	
Sb1_11	1.0994 (10)	1.1171 (3)	0.6883 (4)	0.00971 (9)*	
Sb1_12	1.3815 (10)	0.6263 (3)	0.7864 (4)	0.00971 (9)*	
Sb1_13	1.3883 (10)	1.1249 (3)	0.4501 (4)	0.00971 (9)*	
Sb1_14	1.3832 (10)	0.8785 (3)	0.6191 (4)	0.00971 (9)*	
Sb1_15	1.3809 (11)	1.3726 (3)	0.2806 (4)	0.00971 (9)*	
Sb1_16	1.8855 (9)	0.6279 (3)	0.6190 (4)	0.00971 (9)*	
Sb1_17	1.8806 (7)	0.8751 (3)	0.4514 (3)	0.00971 (9)*	
Sb1_18	0.8855 (10)	1.1202 (3)	0.6137 (4)	0.00971 (9)*	
Sb1_19	0.8903 (10)	0.6142 (3)	0.9527 (4)	0.00971 (9)*	
Sb1_20	1.3802 (10)	0.8715 (2)	0.2841 (4)	0.00971 (9)*	
Sb1_21	0.8828 (10)	1.3689 (2)	0.4531 (4)	0.00971 (9)*	
Sb1_22	1.3795 (10)	0.3758 (3)	0.6173 (4)	0.00971 (9)*	
Sb1_23	1.8835 (10)	1.1273 (3)	0.2857 (4)	0.00971 (9)*	
Sb1_24	1.6034 (10)	0.3755 (3)	0.6894 (4)	0.00971 (9)*	
Sb2_1	1.8145 (10)	0.5380 (3)	0.7707 (4)	0.00914 (9)*	
Sb2_2	1.6734 (10)	0.7147 (3)	0.7069 (4)	0.00914 (9)*	
Sb2_3	1.4954 (10)	0.9490 (3)	0.4858 (4)	0.00914 (9)*	

1	Sb2_4	1.3194 (10)	1.2828 (3)	0.4412 (4)	0.00914 (9)*	
2	Sb2_5	1.3191 (10)	0.7144 (3)	0.6113 (4)	0.00914 (9)*	
3	Sb2_6	1.8140 (10)	0.9630 (3)	0.6022 (4)	0.00914 (9)*	
4	Sb2_7	1.4896 (9)	0.5437 (2)	0.9869 (4)	0.00914 (9)*	
5	Sb2_8	2.1679 (10)	0.5343 (3)	0.8671 (4)	0.00914 (9)*	
6	Sb2_9	1.9871 (10)	0.8046 (3)	0.6537 (4)	0.00914 (9)*	
7	Sb2_10	1.3206 (9)	0.7924 (2)	0.7659 (4)	0.00914 (9)*	
8	Sb2_11	1.3225 (10)	1.2098 (3)	0.6043 (4)	0.00914 (9)*	
9	Sb2_12	1.9915 (10)	0.6942 (3)	0.8209 (4)	0.00914 (9)*	
10	Sb2_13	1.9927 (10)	1.2974 (3)	0.3223 (4)	0.00914 (9)*	
11	Sb2_14	1.4922 (10)	0.5572 (2)	0.6519 (4)	0.00914 (9)*	
12	Sb2_15	0.9941 (10)	1.1981 (3)	0.4884 (4)	0.00914 (9)*	
13	Sb2_16	2.1726 (10)	0.5430 (3)	0.5407 (4)	0.00914 (9)*	
14	Sb2_17	1.6776 (10)	0.7822 (2)	0.5385 (4)	0.00914 (9)*	
15	Sb2_18	1.2949 (9)	0.7162 (2)	0.9470 (4)	0.00914 (9)*	
16	Sb2_19	1.4859 (9)	1.0492 (3)	0.6524 (4)	0.00914 (9)*	
17	Sb2_20	1.4967 (10)	0.4528 (3)	0.8180 (4)	0.00914 (9)*	
18	Sb2_21	1.8176 (10)	1.0415 (2)	0.4362 (4)	0.00914 (9)*	
19	Sb2_22	1.6831 (9)	0.7830 (2)	0.8674 (4)	0.00914 (9)*	
20	Sb2_23	1.4906 (10)	1.0496 (3)	0.3188 (4)	0.00914 (9)*	
21	Sb2_24	2.1639 (10)	0.9674 (3)	0.6971 (4)	0.00914 (9)*	
22	Sb2_25	1.6725 (10)	1.2883 (3)	0.5369 (4)	0.00914 (9)*	
23	Sb2_26	1.8005 (9)	0.9594 (2)	0.2740 (4)	0.00914 (9)*	
24	Sb2_27	1.8254 (10)	0.4678 (3)	0.9445 (4)	0.00914 (9)*	
25	Sb2_28	0.9950 (10)	1.3031 (3)	0.6531 (4)	0.00914 (9)*	
26	Sb2_29	1.4973 (10)	1.4476 (3)	0.4870 (4)	0.00914 (9)*	
27	Sb2_30	2.1755 (9)	0.9636 (2)	0.3720 (4)	0.00914 (9)*	
28	Sb2_31	1.8169 (10)	0.4633 (3)	0.6039 (4)	0.00914 (9)*	
29	Sb2_32	2.1675 (10)	0.4685 (3)	0.7005 (4)	0.00914 (9)*	
30	Sb2_33	2.1574 (9)	1.0315 (3)	0.5308 (4)	0.00914 (9)*	

1	Sb2_34	1.6825 (10)	1.2117 (3)	0.7008 (4)	0.00914 (9)*	
2	Sb2_35	1.6724 (10)	1.2105 (3)	0.3682 (4)	0.00914 (9)*	
3	Sb2_36	1.8146 (10)	1.0385 (3)	0.7746 (4)	0.00914 (9)*	
4	Cd1_1	1.5635 (10)	0.7963 (3)	0.7566 (4)	0.01184 (7)*	
5	Cd1_2	2.1002 (10)	0.7248 (3)	0.7307 (4)	0.01184 (7)*	
6	Cd1_3	2.0592 (10)	0.5506 (3)	0.7592 (4)	0.01184 (7)*	
7	Cd1_4	1.6154 (11)	0.9725 (3)	0.4001 (4)	0.01184 (7)*	
8	Cd1_5	1.5690 (11)	1.2043 (3)	0.5901 (4)	0.01184 (7)*	
9	Cd1_6	1.7726 (10)	0.6485 (3)	0.7918 (4)	0.01184 (7)*	
10	Cd1_7	2.0572 (10)	1.0458 (3)	0.4222 (4)	0.01184 (7)*	
11	Cd1_8	1.6189 (11)	0.5202 (3)	0.9020 (4)	0.01184 (7)*	
12	Cd1_9	1.1108 (10)	1.2736 (3)	0.5645 (4)	0.01184 (7)*	
13	Cd1_10	2.0588 (10)	0.9515 (3)	0.5902 (4)	0.01184 (7)*	
14	Cd1_11	1.6095 (10)	1.0262 (3)	0.5621 (4)	0.01184 (7)*	
15	Cd1_12	1.7657 (11)	0.8539 (3)	0.6272 (4)	0.01184 (7)*	
16	Cd1_13	1.7667 (10)	1.1466 (3)	0.4604 (4)	0.01184 (7)*	
17	Cd1_14	1.6052 (10)	0.4772 (3)	0.7275 (4)	0.01184 (7)*	
18	Cd1_15	1.4185 (10)	0.6997 (3)	0.7182 (4)	0.01184 (7)*	
19	Cd1_16	1.8692 (11)	0.7752 (3)	0.7410 (4)	0.01184 (7)*	
20	Cd1_17	1.5718 (10)	0.7945 (3)	0.4318 (4)	0.01184 (7)*	
21	Cd1_18	1.2527 (10)	1.0928 (3)	0.6215 (4)	0.01184 (7)*	
22	Cd1_19	1.3769 (10)	0.4753 (3)	0.9088 (4)	0.01184 (7)*	
23	Cd1_20	1.5646 (10)	1.2907 (3)	0.4292 (4)	0.01184 (7)*	
24	Cd1_21	1.3786 (10)	1.0205 (3)	0.4121 (4)	0.01184 (7)*	
25	Cd1_22	1.2561 (10)	0.5872 (2)	0.9637 (4)	0.01184 (7)*	
26	Cd1_23	1.0672 (10)	0.5431 (3)	1.0977 (4)	0.01184 (7)*	
27	Cd1_24	2.2746 (10)	0.6079 (3)	0.6310 (4)	0.01184 (7)*	
28	Cd1_25	1.2759 (11)	1.3942 (3)	0.4591 (4)	0.01184 (7)*	
29	Cd1_26	1.7579 (10)	1.3484 (3)	0.2862 (4)	0.01184 (7)*	
30	Cd1_27	2.2815 (10)	0.8932 (3)	0.4647 (4)	0.01184 (7)*	

1	Cd1_28	0.8713 (11)	1.2241 (3)	0.5735 (4)	0.01184 (7)*	
2	Cd1_29	2.1168 (11)	1.2258 (3)	0.4024 (4)	0.01184 (7)*	
3	Cd1_30	1.7141 (10)	0.6054 (3)	0.6828 (4)	0.01184 (7)*	
4	Cd1_31	1.9173 (11)	0.5435 (3)	0.8771 (4)	0.01184 (7)*	
5	Cd1_32	2.1222 (10)	0.7778 (3)	0.5692 (4)	0.01184 (7)*	
6	Cd1_33	1.3695 (10)	0.9761 (3)	0.5711 (4)	0.01184 (7)*	
7	Cd1_34	1.9114 (10)	0.9537 (3)	0.3821 (4)	0.01184 (7)*	
8	Cd1_35	1.2122 (11)	1.1433 (3)	0.5122 (4)	0.01184 (7)*	
9	Cd1_36	2.2116 (10)	0.6425 (3)	0.8510 (4)	0.01184 (7)*	
10	Cd1_37	1.7154 (10)	0.8935 (3)	0.5165 (4)	0.01184 (7)*	
11	Cd1_38	1.3715 (11)	0.5282 (3)	0.7385 (4)	0.01184 (7)*	
12	Cd1_39	1.9138 (10)	0.4607 (3)	0.7106 (4)	0.01184 (7)*	
13	Cd1_40	1.4199 (11)	1.2975 (3)	0.5487 (4)	0.01184 (7)*	
14	Cd1_41	1.6122 (11)	0.9738 (3)	0.7342 (4)	0.01184 (7)*	
15	Cd1_42	1.8736 (10)	1.2664 (3)	0.4129 (4)	0.01184 (7)*	
16	Cd1_43	2.2105 (11)	0.8567 (3)	0.6806 (4)	0.01184 (7)*	
17	Cd1_44	1.9139 (10)	1.0409 (3)	0.5429 (4)	0.01184 (7)*	
18	Cd1_45	1.0651 (11)	1.4503 (3)	0.5920 (4)	0.01184 (7)*	
19	Cd1_46	1.2304 (10)	0.6545 (3)	0.5238 (4)	0.01184 (7)*	
20	Cd1_47	1.1227 (10)	0.7244 (3)	1.0681 (4)	0.01184 (7)*	
21	Cd1_48	1.2311 (10)	1.3450 (3)	0.3490 (4)	0.01184 (7)*	
22	Cd1_49	2.2636 (10)	1.1038 (3)	0.2902 (4)	0.01184 (7)*	
23	Cd1_50	1.0628 (10)	1.0397 (3)	0.7629 (4)	0.01184 (7)*	
24	Cd1_51	1.3839 (10)	0.5214 (3)	1.0806 (4)	0.01184 (7)*	
25	Cd1_52	1.7146 (10)	0.8900 (3)	0.1839 (4)	0.01184 (7)*	
26	Cd1_53	1.4226 (11)	1.2031 (3)	0.3814 (4)	0.01184 (7)*	
27	Cd1_54	1.7571 (10)	0.8392 (3)	0.2948 (4)	0.01184 (7)*	
28	Cd1_55	1.7707 (10)	0.3493 (3)	0.6286 (4)	0.01184 (7)*	
29	Cd1_56	1.7385 (10)	0.4079 (3)	0.8564 (4)	0.01184 (7)*	
30	Cd1_57	1.7153 (11)	1.1034 (3)	0.3492 (4)	0.01184 (7)*	

1	Cd1_58	1.8678 (11)	1.2270 (3)	0.2407 (4)	0.01184 (7)*	
2	Cd1_59	1.9093 (10)	0.9604 (3)	0.7092 (4)	0.01184 (7)*	
3	Cd1_60	1.3830 (10)	0.4791 (3)	0.5771 (4)	0.01184 (7)*	
4	Cd1_61	1.7145 (10)	1.3953 (3)	0.5174 (4)	0.01184 (7)*	
5	Cd1_62	1.9246 (10)	0.5459 (3)	0.5540 (4)	0.01184 (7)*	
6	Cd1_63	1.7324 (10)	1.0960 (3)	0.6808 (4)	0.01184 (7)*	
7	Cd1_64	1.4315 (10)	0.8005 (3)	0.5531 (4)	0.01184 (7)*	
8	Cd3_1	0.9614 (9)	1.2057 (3)	0.7031 (4)	0.0041 (3)*	0.836 (3)
9	Cd3_2	0.5007 (9)	1.3497 (3)	0.7765 (4)	0.0041 (3)*	0.836 (3)
10	Cd3_3	1.0450 (10)	1.2938 (3)	0.7696 (4)	0.0041 (3)*	0.836 (3)
11	Cd3_4	1.2582 (9)	1.1997 (2)	0.7142 (4)	0.0041 (3)*	0.836 (3)
12	Cd3_5	1.5004 (9)	1.1465 (2)	0.7043 (4)	0.0041 (3)*	0.836 (3)
13	Cd3_6	0.4658 (9)	1.2754 (2)	0.6948 (4)	0.0041 (3)*	0.836 (3)
14	Cd3_7	0.7761 (10)	1.2757 (3)	0.7895 (4)	0.0041 (3)*	0.836 (3)
15	Cd3_8	1.0414 (10)	0.7067 (3)	0.9408 (4)	0.0041 (3)*	0.836 (3)
16	Cd3_9	1.4547 (10)	1.4556 (3)	0.3702 (4)	0.0041 (3)*	0.836 (3)
17	Cd3_10	1.5196 (9)	0.6517 (2)	0.9520 (4)	0.0041 (3)*	0.836 (3)
18	Cd3_11	1.4528 (9)	0.8474 (3)	0.8538 (4)	0.0041 (3)*	0.836 (3)
19	Cd3_12	1.4659 (9)	0.7251 (2)	0.8634 (4)	0.0041 (3)*	0.836 (3)
20	Cd3_13	1.2497 (9)	0.7987 (2)	0.8785 (4)	0.0041 (3)*	0.836 (3)
21	Cd3_14	1.2711 (9)	0.5312 (2)	0.4512 (4)	0.0041 (3)*	0.836 (3)
22	Cd2_1	0.527 (4)	1.3220 (15)	0.7817 (15)	0.021 (3)*	0.164 (3)
23	Cd2_2	1.379 (3)	1.2755 (12)	0.7222 (13)	0.021 (3)*	0.164 (3)
24	Cd2_3	0.951 (3)	1.2668 (12)	0.7228 (13)	0.021 (3)*	0.164 (3)
25	Cd2_4	1.031 (3)	1.2274 (12)	0.7788 (13)	0.021 (3)*	0.164 (3)
26	Cd2_5	-1.498 (3)	0.6780 (14)	-0.0718 (14)	0.021 (3)*	0.164 (3)
27	Cd2_6	0.387 (3)	0.8133 (12)	0.8466 (14)	0.021 (3)*	0.164 (3)
28	Cd2_7	0.225 (3)	0.5027 (12)	0.3892 (13)	0.021 (3)*	0.164 (3)
29	Cd2_8	0.199 (4)	0.7733 (17)	0.8593 (17)	0.021 (3)*	0.164 (3)

- 
- 1  
2  
3     <sup>i</sup> Caillat, T.; Fleurial, J.-P.; Borshchevsky, A. *J. Phys. Chem. Solids* **1997**, *58*, 1119.  
4     <sup>ii</sup> Snyder, G. J.; Christensen, M.; Nishibori, E.; Caillat, T.; Iversen, B. B. *Nat. Mater.* **2004**, *3*, 458.  
5     <sup>iii</sup> Nylen, J.; Andersson, M.; Lidin, S.; Häussermann, U. *J. Am. Chem. Soc.* **2004**, *126*, 16306.  
6     <sup>iv</sup> Nylen, J.; Lidin, S.; Andersson, M.; Iversen, B. B.; Liu, H. X.; Newman, N.; Häussermann, U. *Chem. Mater.*  
7     **2007**, *19*, 834.  
8     <sup>v</sup> Nylen, J.; Lidin, S.; Andersson, M.; Liu, H.; Newman, N.; Häussermann, U. *J. Solid State Chem.* **2007**, *180*,  
9      2603.  
10     <sup>vi</sup> Cui JL, Mao LD, Chen DY, Liu XL, Yang W, *Current Appl. Physics* **2009**, *9*, 713-716  
11     <sup>vii</sup> Pedersen, B.L. Birkedal, H., Nygren, M. Fredriksen, P.T and Iversen B.B, *J Appl. Phys.* **2009**, *105*, 013517  
12     <sup>viii</sup> Nakamoto G, Kinoshita K, Kurisu M, *J Appl Phys*, **2009**, *105*, 013713  
13     <sup>ix</sup> Litvinchuk AP, Nylen J, Lorenz B, Guloy, AM and Häussermann, U. *J. Appl Phys.* **2008**, *103*, 123524  
14     <sup>x</sup> Tengå, A.; Lidin, S.; Belieres, J.-P.; Newman, N.; Yang, W. and Häußermann, U. *JACS, asap* **2009**  
15     <sup>xi</sup> Petricek, V., Dusek, M. And Palatinus, L. Institute of Physics, Academy of Sciences of the Czech Republic,  
16 Praha, **2005**  
17     <sup>xii</sup> Zelinska, O. Y.; Bie, H. Y.; Mar, A. *Chem. Mater.* **2007**, *19*, 1518.
- 18  
19  
20  
21  
22  
23  
24  
25  
26  
27  
28  
29  
30  
31  
32  
33  
34  
35  
36  
37  
38  
39  
40  
41  
42  
43  
44  
45  
46  
47  
48  
49  
50  
51  
52  
53  
54  
55  
56  
57  
58  
59  
60

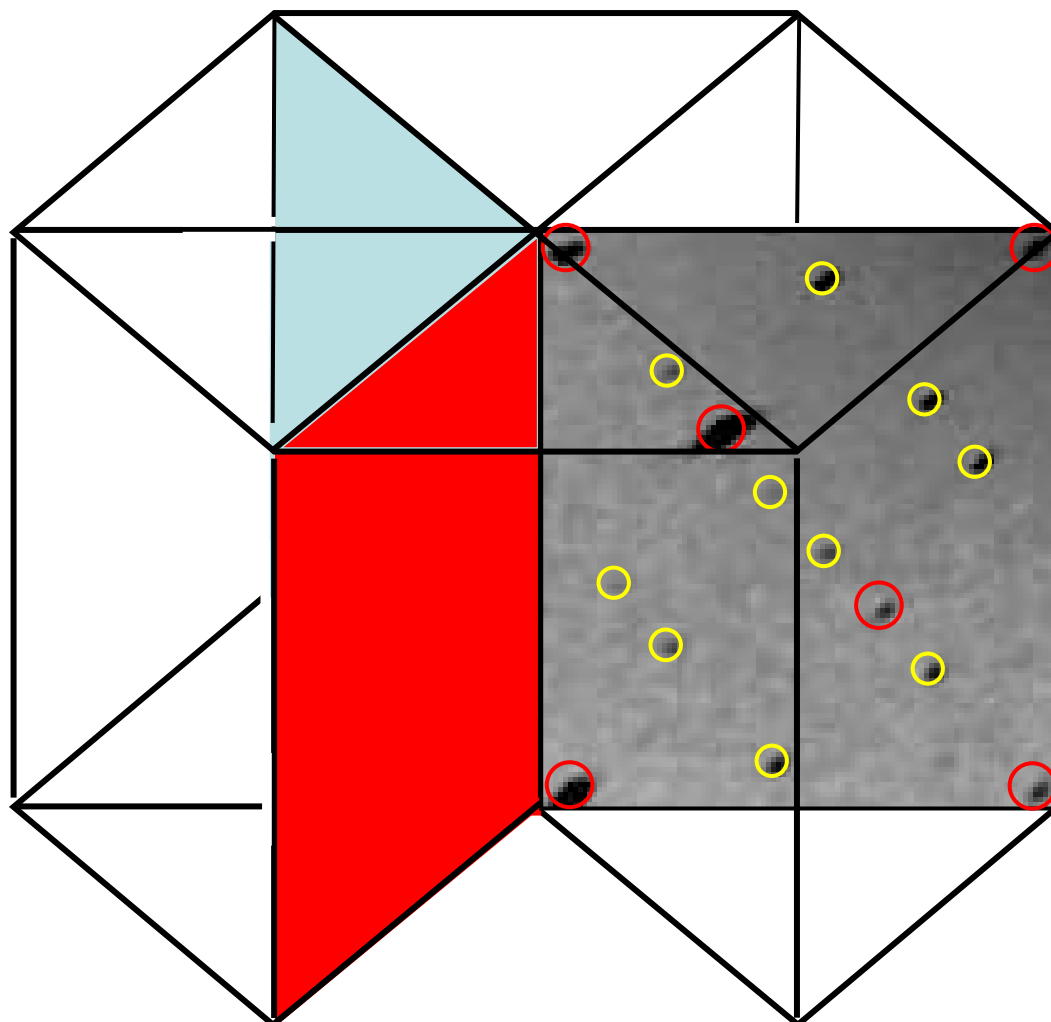


Fig 1

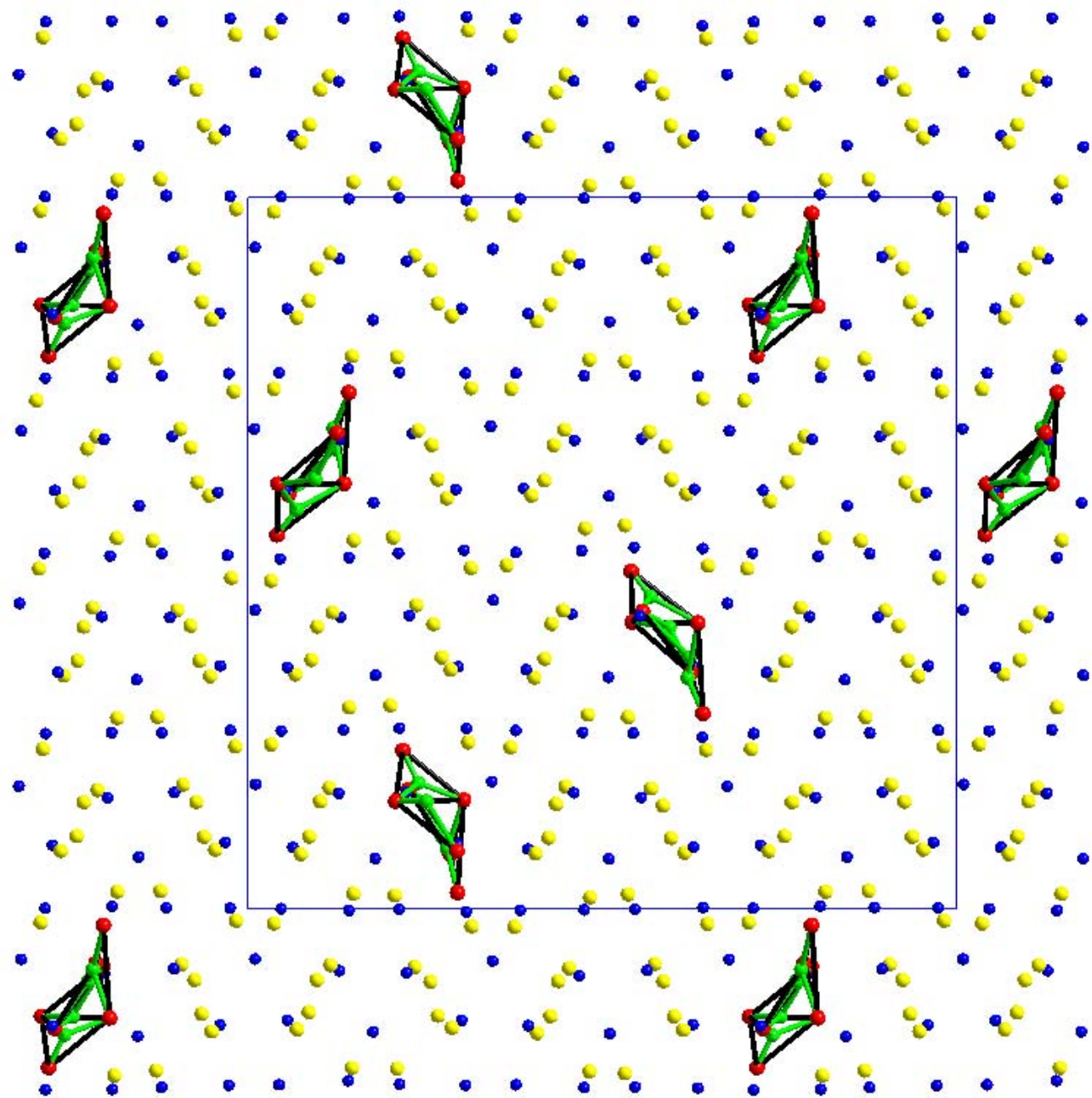


Fig 2a

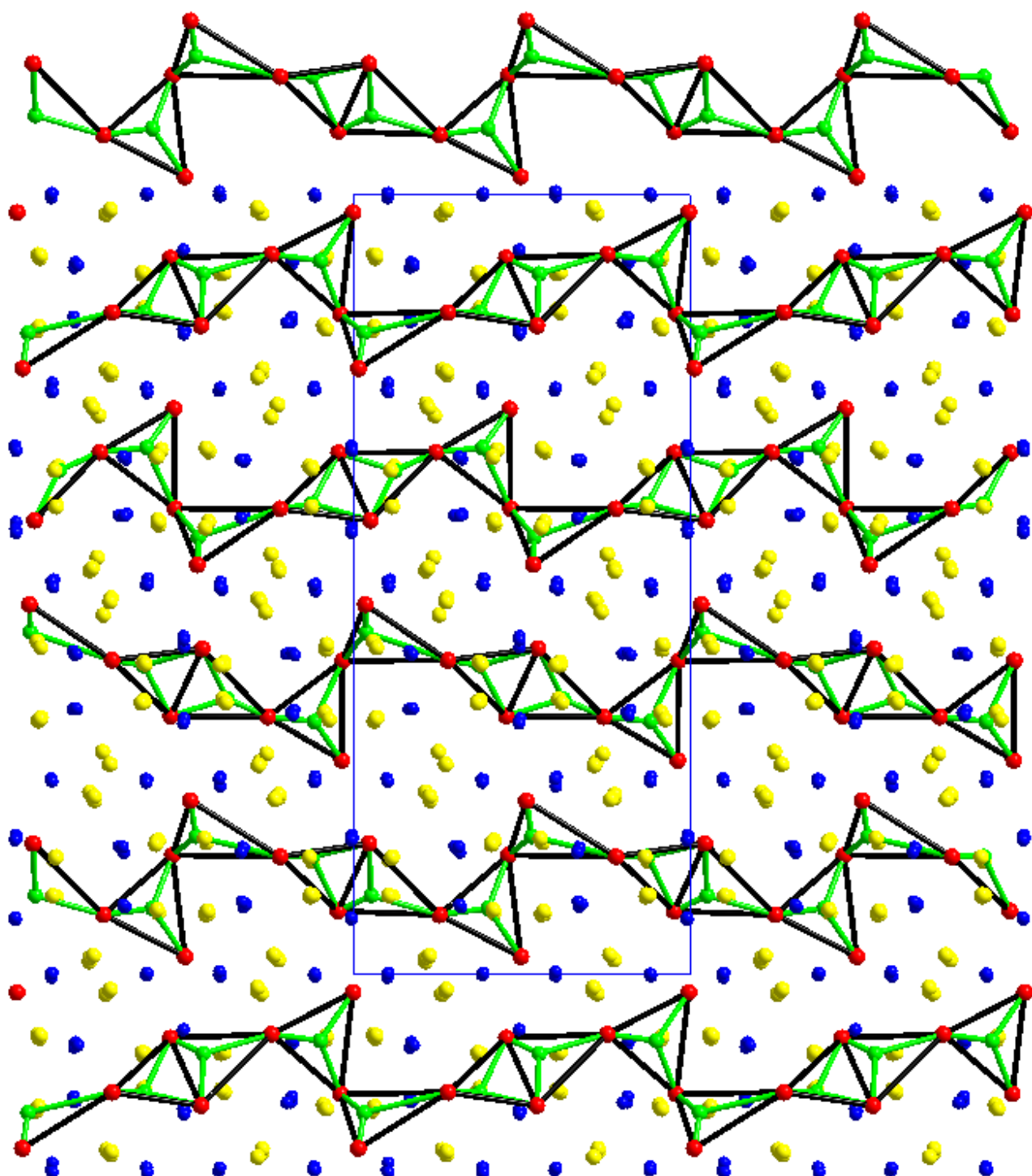


Fig2b

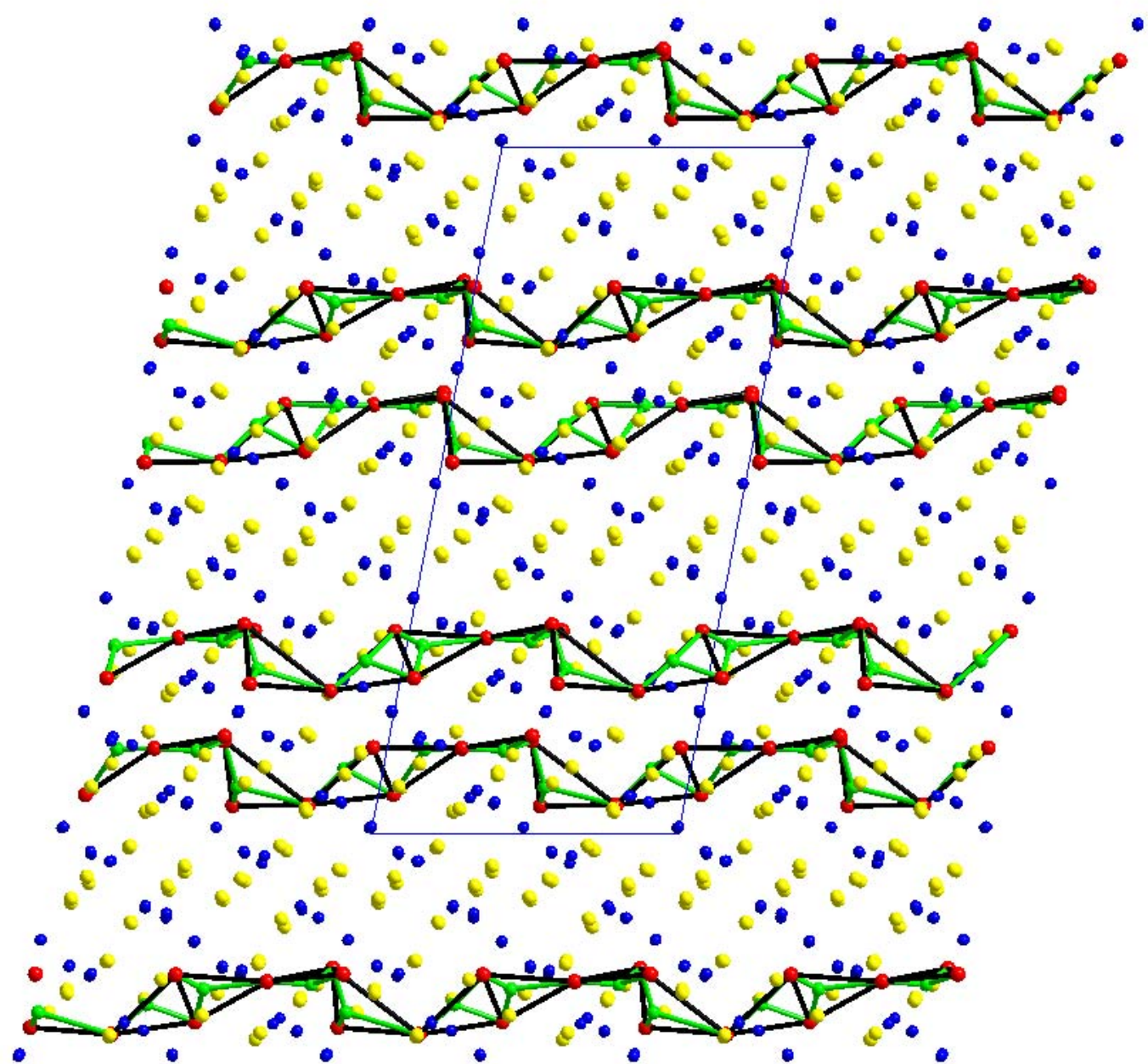


Fig 2c

1  
2  
3  
4  
5  
6  
7  
8  
9  
10  
11  
12  
13  
14  
15  
16  
17  
18  
19  
20  
21  
22  
23  
24  
25  
26  
27  
28  
29  
30  
31  
32  
33  
34  
35  
36  
37  
38  
39  
40  
41  
42  
43  
44  
45  
46  
47  
48  
49  
50  
51  
52  
53  
54  
55  
56  
57  
58  
59  
60